*Journal of Materials Science Research and Reviews*

***1(4): 155-168, 2018; Article no.JMSRR.43664***

# Nitrate Electrochemical Reduction Using Modified Boron- Doped Diamond Electrode from Copper Electroless

**A. B. Couto[1], C. F. Pereira[1] and N. G. Ferreira[1*]**

*[1]Laboratório Associado de Sensores e Materiais, Instituto Nacional de Pesquisas Espaciais – INPE, Av. dos Astronautas 1758, 12227-010 - São José dos Campos, São Paulo, Brasil.*

***Authors' contributions***

*This work was carried out in collaboration between all authors. Author ABC was the intellectual mentor of this study, performed the interpretation of data and wrote the first drafting of the manuscript. Author CFP was responsible for the experimental data acquisition. Author NGF managed the literature searches, guide the research design, revised the paper critically. All authors read and approved the final manuscript.*

***Article Information***

DOI: 10.9734/JMSRR/2018/43664
Editor(s):
(1) Dr. Pernita Dogra, Professor, Department of Chemistry, Maharishi Markandeshwar University, Mullana, India.
(2) Dr. Oscar Jaime Restrepo Baena, Professor, Department of Materials and Minerals, School of Mines, Universidad Nacional de Colombia, Colombia.
Reviewers:
(1) Yongchun Zhu, Shenyang Normal University, China.
(2) Joel Obed Herrera Robles, Autonomous University of Ciudad Juarez, Mexico.
(3) Lyly Nyl Ismail, Universiti Teknologi MARA, Malaysia.
Complete Peer review History: http://www.sciencedomain.org/review-history/26746

***Original Research Article***

***Received 31 July 2018***
***Accepted 02 October 2018***
***Published 22 October 2018***

## ABSTRACT

Modified boron- doped diamond (BDD) electrodes from copper (Cu) electroless process were produced and characterised aiming their application at nitrate electrochemical removal. Cu deposits on BDD surface may promote its conductivity and selectivity increase mainly for nitrate ions reduction using the flow electrochemical reactor. Cu/BDD composites were obtained with optimised parameters to produce high- quality electrodes in suitable doping level associated with Cu particle deposits. BDD films were grown on titanium (Ti) substrates from hot filament chemical vapour deposition reactor. Higher deposit density as well as better Cu particles uniformity was observed for the highest doped BDD electrodes. Considering the nitrate reduction, four cathode and four anode electrodes with 2.5 × 2.5 $cm^2$ were necessary for each electrolysis. The experiments were carried out by varying current density, reactor flow rate, and supporting electrolyte. The process effectiveness was analysed as a function of BDD/Ti and/or Cu/BDD/Ti

**Corresponding author: Email: neidenei.ferreira@inpe.br;*

electrodes as cathode where the results were monitored by Ion Chromatography. This analyses showed the highest electrolysis efficiency for 300 L $h^{-1}$ flow rates, when BDD/Ti electrodes were used both as an anode and as cathode simultaneously. These results were corroborated by X-ray photoelectron spectroscopy (XPS) measurements for electrode surfaces before and after the electrolysis. This behaviour may be associated with the lower impurity adsorption on the film surface due to the turbulent regime used in the flow reactor. On the other hand, when Cu/BDD/Ti was used as a cathode, the best efficiency was obtained for the flow rate of 50 L $h^{-1}$, which may be associated to the low hydrogen adsorption on the electrode surface due to the Cu presence.

*Keywords: Electroless; copper; nitrate; reduction; reactor.*

## 1. INTRODUCTION

Drinking water quality in the world has been directly affected by anthropogenic factors [1]. In addition to the problem of the availability of potable water availability, there is a pollution issue by wastewater discarded from households, commercial establishments, and industry through sanitary sewers. It is possible to observe the impacts generated by the contamination of water resources throughout society as well as public health [2], affecting mainly the places where water does not receive any treatment. Among the materials found as contaminants of the groundwater source, nitrate ion can cause a significant environmental problem. It is generated due to the use of fertiliser products containing large concentrations of nitrogen compounds in addition to inorganic and animal manure, in plantations, soil cultivation, sewage deposited in septic systems, and atmospheric deposition [3]. A recent concern is the increase of nitrate ion levels in drinking water. Particularly, in healthy water in rural areas, the main source of this nitrate is caused by leaching out of cultivated land to rivers and water streams, which can contaminate large areas [4]. The consumption of high concentrations of nitrate ion through water supply is associated with two adverse health effects: the induction to methemoglobinemia [5] and the potential formation of carcinogenic nitrosamines and nitrosamides [6]. Diseases related to the lack of water treatment are a reality, thus, to solve these problems, many papers have been developed to improve the quality of water in lakes, rivers, aquifers, and management as discussed in an analysis between the Brazilian circumstance and the world water development [7].

There are different studies that attempted to remove nitrate from water, which used different techniques such as biological treatment [8], ion exchange [9], reverse osmosis [10], heterogeneous catalysis [11], and electrochemistry [12-15]. Among them, electrochemical technology has been shown to be an excellent nitrate removal technique because it has advantages such as relatively low cost, safe technique, small areas for plant implantation, and environmentally correct procedure due to the use of electron exchange in the electrochemical reduction/oxidation processes. It is important to point out that this technique is strongly influenced by the type of electrode, type of catalyst, pH, and hydrogen flow rate [4]. Concerning the electrochemically-induced nitrate reduction, the cathode material is determinant in this technology efficiency and many metals have already been studied as cathodes like Cu, Fe, Al, Ni, Zn, Ag, Au, Pt and Pd [16-20]. Among them, Cu and Fe have demonstrated to be the very promising material due to their high efficiency and low cost.

In addition, boron- doped diamond (BDD) has been extensively used as electrode material due to its peculiar properties including wide potential window, which allows it to work in cathodic and anodic region extremes, corrosion resistance, high electrical and thermal conductivity, low background current, and high chemical inertia [21], particularly with high efficiency for nitrate removal [22-25]. Recently, Rajic et al. [4] has discussed the complex process concern to the electro-reduction of nitrate at the cathode which starts with nitrate ion absorption. Similarly, Kalaruban et al. [9] have shown the possible reactions at the cathode and at the anode where the oxygen evolution is the main anodic reaction. By using an undivided electrolytic cell, Govindan et al. [26] have studied the mechanism for nitrate removal where nitrite and ammonia are the main products formed during the electrochemical process. They explained the understanding of this mechanism associated with the formation of ammonia from nitrate and nitrite at the cathode and subsequent re-oxidation of ammonia to nitrogen on the catalytic anode surfaces. Their results followed the same trend as discussed by

Perez et al. [21] who used BDD electrodes in the absence of chloride ions.

Also, in previous paper, the reactions occurred anodically on BDD electrode enhancing $^{\bullet}OH$ production [27]. Following this reaction, it is supposed that at the beginning of electrolysis the formation of low $NH_4^+$ may be due to the high quantity of hydroxyl radicals generated on BDD anode, which facilitates the direct ammonia oxidation to nitrogen gas. This assumption is consistent with that reported by Ghazouani et al. [28]. According to them, the hydroxyl radicals are rapidly produced on BDD anode and reach a maximum after 30 min, then, decreases up to the end of electrolysis.

Taking into account the above discussions as well as previous optimised study in the production and characterisation of Cu/BDD/Ti electrodes at different experimental parameters [29], this manuscript shows the application of these electrodes for nitrate removal using the flow electrochemical reactor. From these previous results concerning the Cu deposits on BDD surface, the present study choses the best Cu/BDD/Ti electrode taking into account the electroless parameter variations for two different BDD doping levels, at three pH solutions, and at three deposition times. Thus, the paper discuss about the nitrate electrochemical reduction improvement using two sets of BDD/Ti as anode and BDD/Ti or Cu/BDD/Ti electrodes as the cathode in the electrochemical flow reactor, at different current densities, flow rates, and different supporting electrolytes. For nitrate reduction, the main nitrogen species that could be formed are $NO_2^-$ and $NH_4^+$ ions, according to the following equations [30]:

$$NO_3^-{}_{(sol)} \leftrightarrow NO_3^-{}_{(ads)} \quad (1)$$

$$NO_3^-{}_{(ads)} + 2e^- + H_2O \rightarrow NO_2^-{}_{(sol)} + 2OH^- \quad (2)$$

$$NO_2^-{}_{(sol)} \leftrightarrow NO_2^-{}_{(ads)} \quad (3)$$

$$NO_2^-{}_{(ads)} + 3e^- + 2H_2O \rightarrow \tfrac{1}{2} N_{2\,(g)} + 4OH^- \quad (4)$$

$$NO_2^-{}_{(ads)} + 6e^- + 6H_2O \rightarrow NH_4^+ + 8OH^- \quad (5)$$

In general, the Ion Chromatography (IC) technique is a versatile analytical method for simultaneously measuring inorganic anions ($NO_3^-$ and $NO_2^-$) and cations ($NH_4^+$) for controlling the rate and formation of these ions in the electrolysis processes. IC is a subdivision of High- Performance Liquid Chromatography (HPLC) that includes all rapid liquid chromatography separations of ions in columns coupled online with detection and quantification in a flow-through detector [31]. Its main advantage over the conventional colourimetric, electrometric, or titrimetric methods is that it provides a single instrumental technique that may be used for their rapid, sequential measurement, not to mention, the elimination of hazardous reagent use [32]. Therefore, these ions were monitored by the ion chromatography technique.

## 2. EXPERIMENTAL

### 2.1 Cu/BDD/Ti Production and Characterisation

Firstly, as already described in a previous paper [29], to optimise the parameters for Cu/BDD/Ti production from the electroless process, BDD films were grown on Ti substrates with a geometric area of 1.0 x 1.0 $cm^2$ and thickness of 0.5 mm by hot filament chemical vapour deposition (HFCVD) technique. To minimise the film/substrate stress and to increase its nucleation rate, BDD coatings were deposited on Ti after pre-treatment in air abrasion with glass beads. They were prepared from methane-hydrogen gas mixture with a pressure of 40 Torr and temperature around 650ºC for 24 h. Boron source was obtained by an additional hydrogen line passing through a bubbler containing $B_2O_3$ dissolved in methanol with a controlled B/C ratio that permitted to produce films with different doping levels (5000 and 15000 ppm B/C). To estimate the B acceptor density of BDD sample, Mott-Schottky plots (MSP) curves were taken in 0.5 mol $L^{-1}$ $H_2SO_4$ for the frequency of 10 kHz, peak to peak potential perturbation of 10 mV, and potential range from 0 to 1.0 V x Ag/AgCl/KCl(sat). Prior to the Cu electroless deposition, the sensitisation on the BDD was achieved using a solution of 40 mL $L^{-1}$ HCl containing 0.04 mol $L^{-1}$ $SnCl_2$ for 5 min and the activation was made using a solution containing $7x10^{-4}$ mol $L^{-1}$ $PdCl_2$ with 2.5 mL $L^{-1}$ HCl for 5 min. Ultrasonic vibration was used for both steps. The electroless Cu deposition was carried out at different times (30, 60, 180 and 2400 s) at room temperature. The bath composition was 0.1 mol $L^{-1}$ $CuSO_4$ + 0.2 mol $L^{-1}$ $KNaC_4H_4O_6$ + 17.5 mL $L^{-1}$ HCHO. pH levels were adjusted to 8, 10 and 12 by the addition of NaOH. Fourier transform infrared (FTIR) spectrometer with attenuated total reflectance (ATR) Model Spectrum 100 from Parkin Elmer equipment was used to monitor the

anchor points associated with the functional groups on BDD surfaces promoted by the pre-treatments. The Cu modified diamond film morphologies were verified from the scanning electron microscopy (SEM) images using a Jeol JSM-5310 microscope and the X-ray Diffraction (XRD) patterns using a PAN analytical model X'Pert Powder diffractometer with the CuKα (λ = 1.54 Å), set at 45 kV and 25 mA, running in the ω/2θ scanning mode with ω = 1° and 2θ from 10 to100°. These morphological and structural characterisations were already described in details in previous paper [29].

Therefore, after the parameter optimisations in this Cu electroless process to produce Cu/BDD/Ti electrodes, BDD/Ti films were grown on Ti with geometric area of 2.5 × 2.5 $cm^2$ and thickness of 1.5 mm following the same experimental procedures, but only in the highest doping level of 15000 ppm B/C. For these samples, the Cu electroless parameters were optimised in a solution pH = 12 and deposition time of 30 s. The best electrode performance was also confirmed by linear sweep voltammetry (LSV) measurements for nitrate reduction using 1 mmol $L^{-1}$ Britton-Robinson (BR) buffer (pH=3) + 0,01 mol $L^{-1}$ $KNO_3$ at a sweeping rate of 50 $mVs^{-1}$ for /CuBDD/Ti electrodes at deposition times of 30,60, and 180 s. LSV and MSP experiments were done using a conventional electrochemical cell and a Potentiostat/Galvanostat 302 Autolab/Metrohn equipment with Pt as a counter and $Ag/AgCl/KCl_{(sat)}$ as reference electrodes, respectively.

## 2.2 Nitrate Reduction Using the Electroctrochemical Flow Reactor

Taking into account the electrochemical nitrate reduction the electrolysis was performed using a adapted and assembled electrochemical flow reactor from a previous paper according to Fig.1 [33]. This reactor comprises two parallel polypropylene plates fitted with four electrodes as anodes (total geometric area 16.6 $cm^2$) and four electrodes as cathodes (total geometric area 16.6 $cm^2$). The reactor was connected to a recirculation system (capacity 2.0 L) through which electrolyte could be supplied at flow rates from 50 L $h^{-1}$ (laminar flow; Re 300) to 300 L $h^{-1}$ (turbulent flow; Re 1900). The experiments were carried out using four BDD/Ti electrodes as anode and four BDD/Ti or Cu/BDD/Ti as a cathode using 800 mL of nitrate solution and electrolysis time for 5 h. Aliquots were taken at times: 0, 15, 30, 45, 60, 75, 90, 105, 120, 150, 180, 210, 240, 270 e 300 min. They were analysed using an Ion Chromatography 850 Profissional Metrhom system with an anions column Metrosep A supp 5 and eluent of 0,003 mol $L^{-1}$ $Na_2CO_3$ + 0.001 mol $L^{-1}$ $NaHCO_3$. For all experiments, the distance between the anodes and cathodes was kept constant at 1.5 cm.

Firstly, the electrolysis was carried out in neutral solution 0.1 mol $L^{-1}$ de $K_2SO_4$ + 100 ppm de $KNO_3$ using BDD/Ti electrodes as cathodes and anodes at two current densities of 20 and 200 mA $cm^{-2}$ for three different flow rates of 50, 100, and 300 L $h^{-1}$. Secondly, from the best current density value, the electrolysis was performed using Cu/BDD/Ti as cathodes and BDD/Ti as anodes for two different flow rates of 50 and 300 L $h^{-1}$. Following the latest configuration of the electrodes, the influence of supporting electrolyte for nitrate removal was also studied. For comparison, the electrolysis was performed using a second solution of 0.1 mol $L^{-1}$ phosphate buffer solution (pH=7) + 100 ppm $KNO_3$ and a third solution of 0.1 mol $L^{-1}$ carbonate buffer solution (pH=10) + 100 ppm $KNO_3$. After each

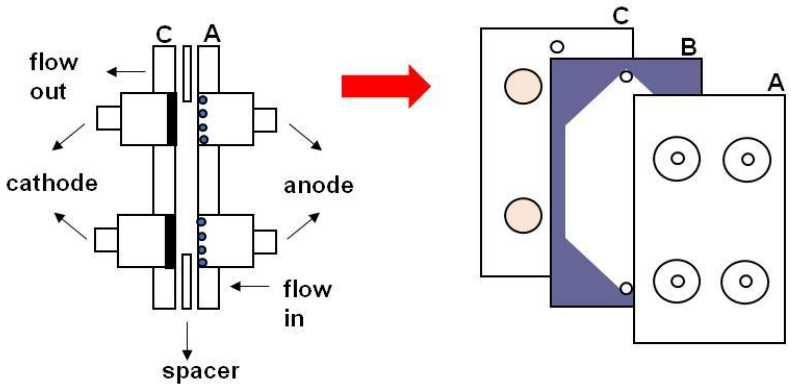


**Fig. 1. Schematic view of the electrochemical flow reactor. A, B, and C represent the external, spacer, and internal parts, respectively.**

electrolysis process, the electrodes were rinsed with isopropyl alcohol in an ultrasound bath. Finally, to evaluate the chemical adsorption on the electrode surfaces after the electrolysis process, the electrode chemical compositions were analysed from X-ray photoelectron spectroscopy (XPS) measurements using a Kratos Axis Ultra XPS system with X-ray Al-Kα (λ = 1486.5 eV).

## 3. RESULTS AND DISCUSSION

### 3.1 Characterisation of BDD/Ti and Cu/BDD/Ti Electrodes

The results of the morphological and structural characterisations of the electrodes used in this paper, through scanning electron microscopy (SEM), Raman spectroscopy, X-ray spectra, and Fourier Transformed Infrared spectroscopy (FTIR) analyses have previously been presented [29]. BDD films completely closed and homogeneous were observed covering the entire substrate considering their roughness morphology. The films did not present cracks or delaminations even after electrolysis experiments. Raman spectra showed high- quality BDD films for both doping levels confirmed by the diamond peak presence in the region of 1332 $cm^{-1}$. The physical meaning of an MSP is the effect of potential E on the thickness of the space-charge layer in the semiconductor. The MSP was used to obtain the boron content on BDD films obtained with different doping levels. Fig 2 depicts this graph for the heavily BDD sample (15000 ppm B/C), with a classical Mott-Schottky behaviour and weak frequency dependence, where the slope of the curve allows determining its acceptor density. The evaluated acceptor density value was 2.42 x $10^{21}$ $B.cm^{-3}$, indicating a heavy doped film with an excellent conductivity and very suitable for electrochemical applications confirming its profile presented in Raman analyses. Concerning the Cu electroless process, the deposits presented small grain morphology distributed all over the diamond crystal faces for both electrodes depending on the electrode boron level, solution pH, and deposition time. Cu metallic crystallographic form was obtained for all depositions. The deposit amounts increased as the pH solution as well as the deposition time increased. SEM images showed a high density of Cu particles for the highest doped BDD electrode. Therefore, from the optimised electroless parameters, the study chose the Cu/BDD/Ti electrodes obtained with pH =12, with the highest doping level, evaluated from Mott-Schottky Plot (MSP), as described above.

The modified Cu/BDD/Ti electrodes at different deposition times were used to evaluate their performance to the nitrate reduction. These analyses were carried out with the purpose of choosing which deposition time presented the greatest performance with respect to the activity and selectivity in the nitrate eletroreduction. These results were important because the best response obtained in these measurements was used as a definining parameter in the electroless deposition time applied to the

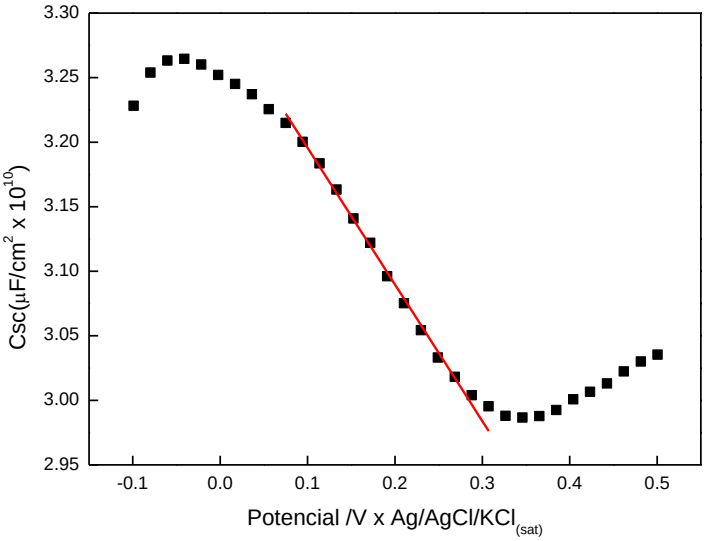


**Fig. 2. MSP curve for the heavily BDD/Ti sample.**

larger electrodes, which were used in the electrochemical flow reactor. Fig. 3 presents linear sweep voltammograms of these electrodes in the presence of nitrate ion as a function of Cu deposition time. For comparison the curve D is related to the Cu/BDD/Ti - 30 s only on BR buffer solution (blank). It was possible to observe that Cu deposited on diamond surface catalyses the electroreduction of nitrate for all electrodes. Nitrate electroreduction is a very complex process. Several products depend on the experimental conditions such as pH and applied potential. In this work, the cathodic peak is observed around -0.6 V x $Ag/AgCl/KCl_{(sat)}$ for the three electrodes studied, suggesting that nitrate to nitrite reduction is taking place at this potential.

As can be observed in Fig. 3(C), despite the high density of Cu particles deposited on the BDD surface with deposition time of 180s (C) [29], it did not increase the catalytic activity for nitrate reduction, since the voltammogram of the nitrate showed a lower cathodic current when compared to those of Cu/BDD/Ti obtained at deposition times of the 30 (A) and 60s (B). A more significant difference was observed in the voltammogram of the Cu/BDD/Ti electrode of 30s of deposition time (A), which showed a peak around -0.6 V x $Ag/AgCl/KCl_{(sat)}$ related to nitrate to nitrite reduction followed by a shoulder around -1.1 V x $Ag/AgCl/KCl_{(sat)}$ relative to the nitrate reduction to ammonia. In addition, a slight increase in cathodic current was observed, showing that the reduction of nitrate was better catalysed in the presence of smaller Cu particle amounts. Therefore, Cu/BDD/Ti-30s electrode presented the best activity and selectivity for both nitrite and ammonia ions in nitrate reduction while Cu/BDD/Ti electrodes obtained at 60 and 180 s deposition times presented activity and selectivity only for nitrite ion. However, it is important to note that the Cu/BDD/Ti-60s showed the largest peak definition related to nitrate to nitrite reduction. Thus, the deposition time of 30 s was chosen for Cu electroless process on larger BDD electrode (2.5 x 2.5 $cm^2$) for using in nitrate removal in the electrochemical flow reactor.

### 3.2 Electrolysis of Nitrate Ions

The study for nitrate removal was performed in a systematic way considering different experimental parameters on the electrochemical flow reactor. Firstly, some criteria were established to impose a range for these parameter variations. Concerning the supporting electrolyte, the neutral medium of $K_2SO_4$ was chosen due to its same cation of the reagent $KNO_3$ decreasing in this way the amount of ions and, consequently, decreasing the probability of peak overlaps for ion chromatography analyses. The study chose two values of current density 20 and 200 $mAcm^{-2}$. The minimum current value was explained by the mass transfer model used to estimate the minimum necessary current to degrade nitrate to obtain nitrite and ammonium as final products [14,15]. Besides, other studies have already discussed the nitrate degradation efficiency in this current range [14, 15, 34]. On the other hand, the second current value was

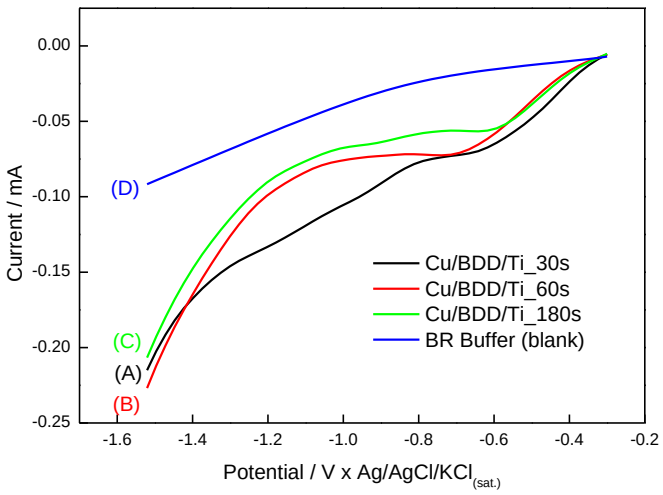


**Fig. 3. LSV response of Cu/BDD/Ti electrodes with deposition times of 30, 60 and 180 s for $10^{-3}$ mol $L^{-1}$ BR buffer solutions (pH=3) and nitrate reduction in a solution of $10^{-2}$ mol $L^{-1}$ $KNO_3$ + $10^{-3}$ mol $L^{-1}$ BR buffer solution (pH=3). Scan rate: 50 mV $s^{-1}$.**

chosen due to studies that have reported good degradation results with higher current values [35,36], and also attributed to the interest in investigating the behaviour of degradation that uses, comparatively, a current ten times greater. Thus, two values of current density, different in one order of magnitude, were defined to investigate a possible proportionality relationship between the current density and the percentage of degraded nitrate.

### 3.2.1 Influence of flow rate and current density

For this purpose, the reactor set up was kept using BDD/Ti electrodes for anodes and for cathodes three flow rates of 50, 100, and 300 L $h^{-1}$ were studied in the two current densities of 20 and 200 mA $cm^{-2}$. For the experiments using 20 mA $cm^{-2}$ the electrolysis results are presented in Fig. 4(a) where all flow rates showed the degradation of part of the pollutant, implying a sharp decrease in the nitrate concentration at the beginning of the experiments, even though this decay rate did not show continuity after the first hour of degradation. For the nitrate reduction, firstly the adsorption of the nitrate should occur on the electrode surface. In aqueous media, the following main reactions (6), (7), (8), (9), may take place at the active sites of the cathode electrode:

$$NO_3^-{}_{(sol)} \leftrightarrow NO_3^-{}_{(ads)} \quad (6)$$

$$H_2O_{ads} \leftrightarrow OH^-_{ads} + H^+_{ads} \quad (7)$$

$$H^+_{ads} + e^- \leftrightarrow H_{ads} \quad (8)$$

$$2H_{ads} \leftrightarrow H_2\uparrow \quad (9)$$

Indeed, on the cathode surface, there is a competition between the nitrate, and the hydrogen reduction. Thus, it is believed that the degradation rate was reduced after the first hour due to the physical adsorption of the hydrogen on the electrode surface, decreasing the interaction between the electrode and the pollutant over time not to mention the possible adsorption of intermediate compounds generated during the degradation. As explained in the experimental part, aliquots were taken during the electrolysis process and the results were analysed by ion chromatography. The obtained values were normalised in all the presented results. The electrolysis of the pollutant at the fluxes of 50 (A) and 100 L $h^{-1}$ (B) was very similar, with nitrate removal of 6 and 7%, respectively. On the other hand, in the flow rate of 300 L $h^{-1}$ (C) the degradation was greater, reducing 13% of the pollutant. As the nitrate reduction values were very close to flow rates of 50 and 100 L $h^{-1}$, it is possible to speculate that the small variation in flow rate was not sufficient to change the laminar flow regime established in the smaller flow rates. In contrast to this result, the significant nitrate removal increase in the flow rate of 300 L $h^{-1}$ was attributed to the lower adsorption of hydrogen particles and/or intermediate products on the electrode surfaces provided by its turbulent fluid flow regime. Considering the nitrate removal experiments for 200 $mAcm^{-2}$, similar results were observed for the flows of 50 (A) and 100 L $h^{-1}$ (B) of 11 and 12%, respectively. Following the same degradation behaviour performed at 20 mA $cm^{-2}$, the best response occurred at the highest flow rate, 300 L $h^{-1}$ (C), reducing 15% of the pollutant, as shown in Fig. 4 (b).

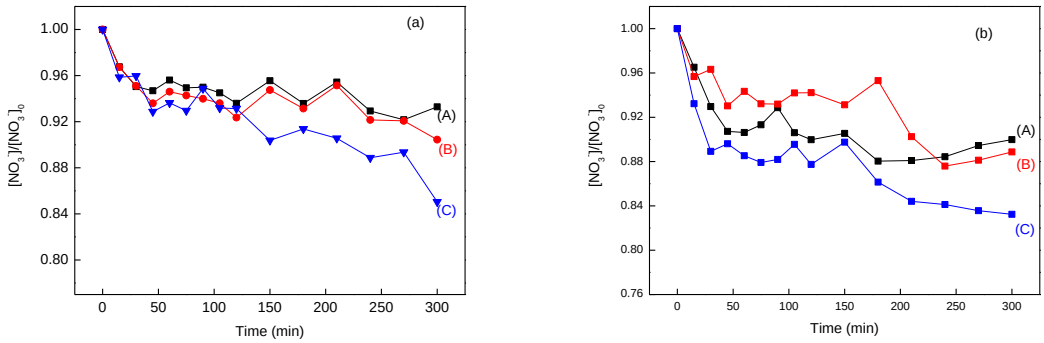


**Fig. 4. Nitrate removal as a function of the electrolysis time for the three flow rates of (A) 50, (B) 100, and (C) 300 L $h^{-1}$. (a) 20 $mAcm^{-2}$; (b) 200 $mAcm^{-2}$.**

To justify the inference of the physical adsorption of intermediate products on the electrode surfaces, the films were analysed by XPS before and after the degradations proving the adsorption of elements on the film surface, especially after a low flux electrolysis. Fig. 5 presents a general evaluation of the chemical composition of all elements on the BDD film surface from the XPS Survey spectra before and after the nitrate ion electrolysis process. The spectrum showed the presence of two main peaks related to C 1s (284.5 eV) and O 1s (529.2 eV) for the BDD film before nitrate ion electrolysis. As can be seen in Fig. 5, the presence of different chemical elements such as N 1s (398.6 eV), K 2p (292.8) and S 2p (164,3 eV) was observed after the nitrate ion electrolysis as possible contaminant elements on the BDD surface. Besides, the C 1s decreased associated with the O 1s peak increase, for both flow rates. These results confirm that there was adsorption of intermediates on the surface of the electrode during the process of nitrate ion reduction. Detailed information on the atomic concentrations of C 1s, O 1s, N 1s, K 2p and S 2p were calculated from the Survey spectra using Kratos Vision software. These results are presented in Table 1.

According to the results of Table 1, there is a higher contaminant percentage when the electrolysis was performed in a 50 L $h^{-1}$ flow rate compared to that performed with a flow rate of 300 L $h^{-1}$. Another significant difference is associated with the C/O ratio on the diamond surface before and after the nitrate ion reduction. There was a larger decrease in this ratio when the electrolysis was performed using a 50 L $h^{-1}$. This behaviour may be related to a possible inhibition of active sites of the BDD electrode, as a consequence, there was a small decrease in the efficiency of the reduction of the nitrate ion using flow rate of 50 L $h^{-1}$. It is believed that the turbulent regime, established in the higher flows, acts by removing the adsorbed particles in the electrode due to the great agitation generated in the displacement of the fluid by the non-linear flow rate of its particles, providing a larger contact surface between the electrode and the nitrate ion. Otherwise, the laminar regime, established in the smallest flow, presents the least agitation in the layers of the fluid during its movement, allowing particles such as hydrogen and/or intermediate products generated during the degradation to remain adsorbed on the electrode.

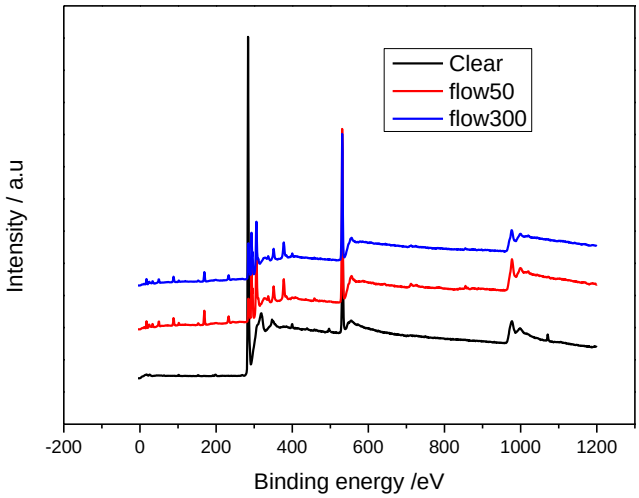


**Fig. 5. XPS Survey spectra before and after the nitrate ion electrolysis process.**

**Table 1. Mass concentration percentage of C 1s, O 1s, N 1s, K 2p, and S 2p obtained from XPS spectra**

| Peak | Before electrolysis % mass conc. | After electrolysis (flow 300) % mass conc. | After electrolysis (flow 50) % mass conc. |
|---|---|---|---|
| C 1s | 85.13 | 23.92 | 12.07 |
| O 1s | 14.87 | 45.05 | 51.94 |
| N 1s | - | 1.11 | - |
| K 2p | - | 22.66 | 26.78 |
| S 2p | - | 7.19 | 9.09 |

These results are coherence when compared to those of degradations carried out with the current density of 20 mA $cm^{-2}$, confirming the tendency of the sharp drop of the pollutant concentration in the electrolysis beginning, although this behaviour does not continue throughout the process. Thus, a trend was observed in the flow rate study with the use of unmodified electrodes: the higher the flow rate the better the efficiency of nitrate removal. Moreover, since a great similarity was observed considering degradation results carried out inflows of 50 and 100 L $h^{-1}$, the study using 100 L $h^{-1}$ was neglected in next steps based on the assumption that the small flow variation between them was not sufficient to change satisfactorily the degradation behaviour.

Concerning the flow rate of 300 L $h^{-1}$, the rates of nitrate concentration decay are considerably different between the two applied current densities, although the final result, in degrading terms, is similar. Nonetheless, a significant drop in nitrate concentration is observed for the three initial times of collection, when the 200 mA $cm^{-2}$ current density is used. However, this effect is greatly reduced for the lower current density. For the total degradation time, the effect of a current density ten times higher is not significant. By comparing the curves (C) on Fig 4 (a) and (b) the nitrate removals were 13 and 15% for current densities of 20 and 200 mA $cm^{-2}$, respectively. Although the nitrate removal was greater in the current density of 200 mA $cm^{-2}$, no proportionality relation was observed in comparison to that of 20 mA $cm^{-2}$. Therefore, the choice of 200 mA $cm^{-2}$ is inappropriate for this study, because there is no linear relationship between the applied current density and the percentage of degraded nitrate [13]. The small increase observed in the degradation rate after a significant increase in energy expenditure may be related to the evolution reaction of hydrogen, which competes with the degradation of nitrate consuming part of the energy supplied to the electrolysis, resulting in a degradation rate of the pollutant lower than that expected [12,13,34,37]. These data are in agreement with other papers where the linear relationship between energy consumption and percentage of degraded nitrate was not observed [13,34]. In addition, these studies also confirmed that the current density of 20 mA $cm^{-2}$ is the best choice.

Also, the specific energy consumption was performed to show that the higher current density is not appropriated according to equation 10:

$$CE = (E.I.t)/1000 \quad (10)$$

where:

E is the potential measured during the electolysis (V);
I is the applied current;
t is the electrolysis time (h).

Thus, the energy consumption may be evaluated from:

$$CEs = CE/\Delta m \quad (11)$$

where Δm is the difference between the initial and final nitrate mass during the electrolysis. These results are presented in Table 2 for the two current densities studied.

Although the values of nitrate degraded mass are similar, the energy used in the electrolysis is totally different. In comparison, the specific energy consumption of the degradation performed using the higher current is more than twenty times greater than that of the lower current. Therefore, there is a strong dependence relation between energy consumption and current density, even if this association is not linear [38]. Taking into account that all parameters such as media resistivity, supporting electrolyte, electrodes, and flow rate were the same in the degradations, it is believed that energy excess was used in the parallel reactions of hydrogen evolution during electrolysis. In order to continue the degradations, the current density of 20 mA $cm^{-2}$ was chosen, since it showed a more suitable relation between the consumed energy and the amount of degraded pollutant.

**Table 2. Relationship between the energy consumption of nitrate degradation at two current densities: 20 and 200 mA $cm^{-2}$**

| Current density (mA $cm^{-2}$) | Removal nitrate mass (g) | Potential E(V) | CE (kWh) | CEs (kWh $g^{-1}$) |
|---|---|---|---|---|
| **20** | $1,515x10^{-2}$ | 5,65 | $7,063x10^{-3}$ | 0,466 |
| **200** | $1,692x10^{-2}$ | 14,52 | $1,836x10^{-1}$ | 10,85 |

### 3.2.2 Influence of Cu/BDD/Ti cathode

After the preceding optimisation parameters, the next step of this work was to apply the modified diamond films through the Cu electroless process as the cathode in the electrolysis process for nitrate removal. According to Lacasa et al. [14], the deposition of a thin layer of copper particles has a catalytic effect on the nitrate degradation, reducing the physical adsorption of hydrogen on the cathodic electrode surface, favouring the pollutant adsorption. To maintain a comparative parameter, the influence of the modified electrodes was studied for flow rates of 50 and 300 L $h^{-1}$ and the current density of 20 mA $cm^{-2}$. The comparison between the electrolysis using BDD/Ti and Cu/BDD/Ti cathodes are shown in Fig. 6 (a) and (b) for flow rates of 300 and 50 L $h^{-1}$, respectively.

The degradation carried out with the modified Cu/BDD/Ti cathode (B) shows a slight improvement in the final value of the degradation in relation to that obtained with the BDD/Ti cathode (A). Nevertheless, the performance of the electrodes was similar during the electrolysis. This behaviour can be attributed to the turbulent regime, which, like copper, inhibits the physical adsorption of hydrogen and/or intermediate products on the electrode surface. Nonetheless, taking into account the previous results where only BDD cathodes were used, the influence of flow rate variation was more significant in the electrolysis results than that for using Cu/BDD/Ti modified cathode. Similar experiments were performed for the lowest flow rate, which presented a notable behaviour (Fig. 6 (b)). The laminar regime, established in the 50 L $h^{-1}$ flow rate, generated the lowest possible stirring during the liquid flow, allowing greater physical adsorption of the substances on the electrode. Thus, in this regime, where the fluid mechanic favoured the greater adsorption of particles in the films, the copper effect as catalytic metal became more expressive. While BDD/Ti (A) cathode showed a marked drop in pollutant concentration only on the end of the first hour, results using the modified Cu/DDB/Ti (B) electrode showed a more continuous decay rate throughout the process, proving the higher nitrate reduction in the lower flow. In this type of fluid flow, regime copper is responsible for the lower adsorption of hydrogen in the electrodes, confirming the catalytic activity of the metal in the nitrate degradation [14,34].

### 3.2.3 Influence of supporting electrolyte

The electrolysis parameter investigations showed up to now the necessity of a systematic study related to this complex process of nitrate removal. Thus, the final parameter studied is related to the supporting electrolyte influence in a solution of phosphate buffer and in carbonate buffer solutions, remembering that up to this stage the medium used as supporting electrolyte was composed of $K_2SO_4$ 0.1 mol $L^{-1}$ and 100 ppm of $KNO_3$. Thus, to avoid conductivity discrepancies between these nitrate diluents, the ionic concentration of two media was maintained at 0.1 mol $L^{-1}$. Also, the initial pH = 7 of phosphate buffer solution was the same to that of sulfate medium, while for carbonate buffer solution the pH = 10. The current density was kept at 20 mA $cm^{-2}$ for a flow rate of 50 L $h^{-1}$. The electrolysis results are depicted in Fig. 7. The first medium studied was sulfate (A). Comparatively, this medium

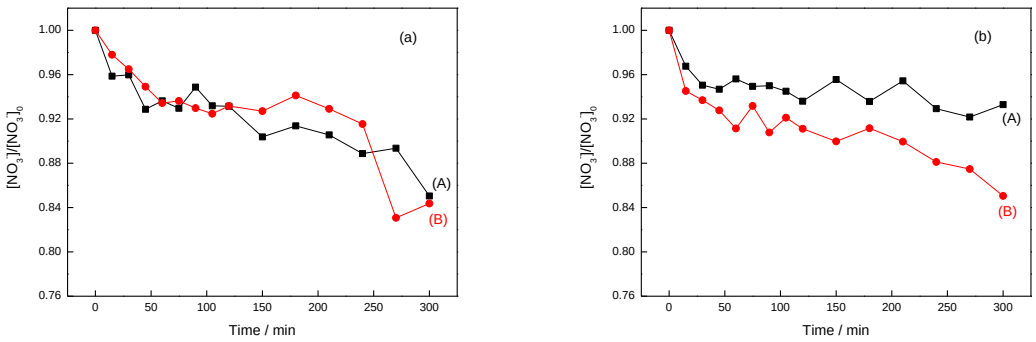


**Fig. 6. Nitrate removal as a function of the electrolysis time using two different cathodes of (A) BDD/Ti and (B) Cu/BDD/Ti. (a) 300 $Lh^{-1}$; (b) 50 L $h^{-1}$.**

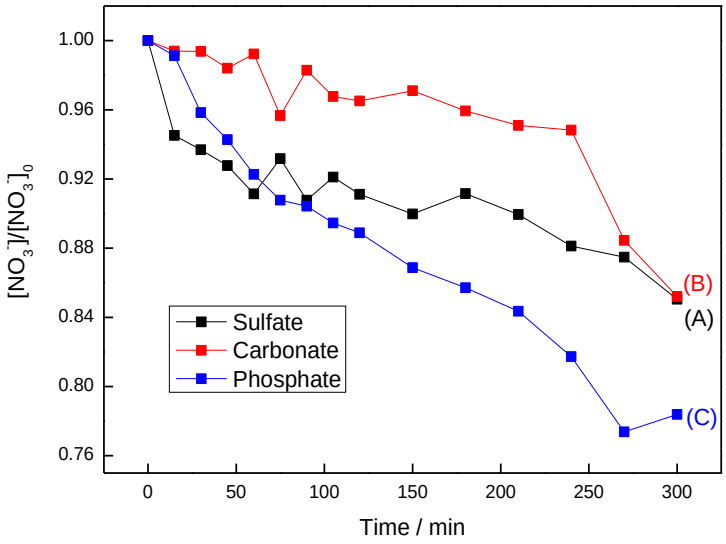


**Fig. 7. Nitrate removal for different supporting electrolytes at 20 mA cm$^{-2}$ and 50 L h$^{-1}$ using Cu/BDD/Ti as cathode. (A) potassium sulfate; (B) carbonate buffer solution; (C) Phosphate buffer solution.**

**Table 3. Relationship among the energy consumption of nitrate degradation in three support electrolyte of sulfate, carbonate buffer, and phosphate buffer**

| Supporting electrolyte | Removal nitrate mass (g) | Potential E(V) | CE (kWh) | CEs (kWh g$^{-1}$) |
|---|---|---|---|---|
| Sulfate | 1.514x10$^{-2}$ | 5.43 | 6.787x10$^{-3}$ | 0.448 |
| Carbonate | 1.493x10$^{-2}$ | 5.97 | 7.462x10$^{-3}$ | 0.499 |
| Phosphate | 2.185x10$^{-2}$ | 8.66 | 10.83x10$^{-3}$ | 0.495 |

showed the greatest drop in the pollutant concentration in the first 50 min of electrolysis. In this range, the carbonate buffer (B) showed the lowest drop while the phosphate buffer solution (C) had an intermediate behaviour. On the other hand, analysing the final degradation, the phosphate buffer solution had the best result, followed by the sulfate solution while the carbonate buffer was the supporting electrolyte with the lowest degradation, very close to that for sulfate electrolyte.

Regarding energy spending, there was a small increase in consumption when the carbonate buffer solution was used in relation to that of sulfate. The latter demonstrated the best relationship between degraded mass and energy consumption. The sulphate solution further degraded comparatively the largest amount of nitrate mass and was able to maintain the specific energy consumption in the level comparable to that for other supporting electrolytes, according to Table 3.

The use of carbonate buffer solution resulted in an increase in energy consumption relative to that of sulfate resulting in its lowest nitrate reduction in terms of degraded mass. Also, the phosphate buffer solution demonstrated an energy spending comparable to that of carbonate buffer solution. Nonetheless, this was the supporting electrolyte that presented the greatest nitrate degradation.

## 4. CONCLUSION

In summary, some parameters of the electrochemical flow reactor were optimised in the study of nitrate electrolysis using BDD/Ti and/or Cu/BDD/Ti as the cathode material. A small increase in electrolysis efficiency was obtained for BDD/Ti in the highest flow rate of 300 L h$^{-1}$ due to its lowest adsorption of impurities on the electrode surface, attributed to the turbulent reactor regime. On the other hand, using Cu/BDD/Ti electrodes in the cathodic region, better results were observed in the lowest flow rate studied, which may be associated to its

lowest hydrogen and/or intermediate products adsorption process in the electrode promoted by Cu. The current density of 20 mA $cm^{-2}$ was most appropriate because no linearity relationship was observed between the increase in applied current density and the percentage of degraded nitrate. Among the evaluated media, the phosphate buffer degraded more pollutants with proportional lower energy expenditure.

## ACKNOWLEDGEMENTS

This paper is a contribution of the Brazilian National Institute of Science and Technology (INCT) for Climate Change funded by CNPq grant number 573797/2008-0. We also thank CAPES and FAPESP (Grant Number 2016/13393-9) for financial support.

## COMPETING INTERESTS

Authors have declared that no competing interests exist.

## REFERENCES

1. Falkenberg LJ, Stian CA. Too much data is never enough: A review of the mismatch between scales of water quality data collection and reporting from recent marine dredging programmes. Ecological Indicators. 2014;45:529-537.
2. Szabo J, Minamyer S. Decontamination of biological agents from drinking water infrastructure: A literature review and summary. Environment International. 2014;72:124-128.
3. Baird C, Cann M. Química Ambiental. Bookman, Porto Alegre; 2011.
4. Rajic Lj, Berroa D, Gregor S, Elbakri S, MacNeil M, Alshawabkeh AN. Electrochemically-induced reduction of nitrate in aqueous solution. International Journal of Electrochemical Science. 2017; 12:5998–6009.
5. Glade MJ. Food, nutrition, and the prevention of cancer: A global perspective. American Institute for Cancer Research/World Cancer Research Fund, American Institute for Cancer Research, 1997. Nutrition. 1999;15(6):523-6.
6. Sisinno CLS. Non-inert industrial solid waste disposal in landfill dumps: evaluation of toxicity and implications for the environment and human health. Caderno de Saúde Pública. 2003;19(2): 369-374.
7. Rego Filho MTN, Braga ACR, Curi CR. A dimensão da disponibilidade hídrica: Uma análise entre a conjuntura brasileira e o relatório de desenvolvimento mundial da água. Ambiência. 2014;10(1):111-124.
8. Winkler M, Coats ER, Brinkman CK. Advancing post-anoxic denitrification for biological nutrient removal. Water Research. 2011;45:6119-6130.
9. Kalaruban M, Loganathan P, Shim WG, Kandasamy J, Naidu G, Nguyen TV, Vigneswaran S. Removing nitrate from water using iron-modified Dowex 21K XLT ion exchange resin: Batch and fluidised-bed adsorption studies. Separation and Purification Technology. 2016;158:62-70.
10. Epsztein R, Nir O, Lahav O, Green M. Selective nitrate removal from groundwater using a hybrid nanofiltration-reverse osmosis filtration scheme. Chemical Engineering Journal. 2015;279:372-378.
11. Thomas JM, Thomas JW. Principles and practice of heteregenous catalysis. Wheinhein, New York; 1997.
12. Reyter D, Bélanger D, Roué L. Nitrate removal by a paired electrolysis on copper and Ti/IrO2 coupled electrodes - influence of the anode/cathode surface area ratio. Water Research. 2010;44:1918-1926.
13. Li M, Feng C, Zhang Z, Yang S, Sugiura N. Treatment of nitrate contaminated water using an electrochemical method. Bioresource Technology. 2010;101:6553-6557.
14. Lacasa E, Cañizares P, Llanos J, Rodrigo MA. Effect of the cathode material on the removal of nitrates by electrolysis in non-chloride media. Journal of Hazardous Materials. 2012;213-214:478-484.
15. Lacasa E, Cañizares P, Llanos J, Rodrigo MA. Electrochermical denitrification with chlorides using DSA and BDD anodes. Chemical Engineering Journal. 2012;184: 66-71.
16. Yang J, Sebastian P, Duca M, Hoogenbooma T, Koper MTM. pH dependence of the electroreduction of nitrate on Rh and Pt polycrystalline electrodes. Chemical Communication. 2014;50:2148-2151.
17. Estudillo-Wong LA, Arce-Estrada EM, Alonso-Vante N, Manzo-Robledo A.

Electro-reduction of nitrate species on Pt-based nanoparticles: Surface area effect. Catalysis Today. 2011;166:201-204.

18. Wang Q, Zhao X, Zhang J, Zhang X. Investigation of nitrate reduction on polycrystalline Pt nanoparticles with controlled crystal plane. Journal Electroanalytical Chemistry. 2015;755:210-214.
19. Su JF, Ruzybayev I, Shah I, Huang CP. The electrochemical reduction of nitrate over micro-architectured metal electrodes with stainless steel scaffold. Applied Catalysis B: Environmental. 2016;180: 199-209.
20. Katsounaros I, Kyriacou G. Influence of nitrate concentration on its electrochemical reduction on tin cathode: Identification of reaction intermediates. Electrochimica Acta. 2008;53:5477-5484.
21. Pérez G, Ibáñez R, Urtiaga AM, Ortiz I. Kinetic study of the simultaneous electrochemical removal of aqueous nitrogen compounds using BDD electrodes. Chemical Engineering Journal. 2012;197:475–482.
22. Reuben C, Galun E, Cohen H, Tenne R, Kalish R, Muraki Y, Hashimoto K, Fujishima A, Butler JM, Lévy-Clément, C. Efficient reduction of nitrite and nitrate to ammonia using thin-film B-doped diamond electrodes. Journal Electroanalytical Chemistry. 1995;396:233–239.
23. Ndao AN, Zenia F, Deneuville A, Bernard M, Lévy-Clément C. Effect of boron concentration on the electrochemical reduction of nitrates on polycrystalline diamond electrodes. Diamond Related Materials. 2000;9:1175–1180.
24. Matsushima JT, Silva WM, Azevedo AF, Baldan MR, Ferreira NG. The influence of boron content on electroanalytical detection of nitrate using BDD electrodes. Applied. Surface Science. 2009;256:757–762.
25. Lévy-Clément C, Ndao NA, Katty A, Bernard M, Deneuville A, Comninellis C, Fujishima A. Boron doped diamond electrodes for nitrate elimination in concentrated wastewater, Diamond Related Materials. 2003;12:606–612.
26. Govindan K, Noela M, Mohan R. Removal of nitrate ion from water by electrochemical approaches. Journal of Water Process Engineering. 2015;6:58–63.
27. Couto AB, Oishi SS, Ferreira NG. Enhancement of nitrate electroreduction using BDD anode and metal modified carbon fiber cathode. Journal of Industrial and Engineering Chemistry. 2016;39:210-217.
28. Ghazouani M, Akrout H, Bousselmi L. Efficiency of electrochemical denitrification using electrolysis cell containingBDD electrode. Desalination and Water Treatment. 2014;53:1-11.
29. Pereira CF, Couto AB, Baldan MR, Ferreira NG. Copper Electroless Process Optimization to Modify Boron Doped Diamond at Different Boron Levels. ECS Transactions. 2015;64:15-22.
30. Yang S, Wang L, Jiao X, Li P. Electrochemical reduction of nitrate on different Cu-Zn oxide composite cathodes. Int. J. Electrochem. Sci. 2017;12:4370-4383.
31. Schwedt G. Trenn- und Anreicherungsmethoden in der anorganischen Anionenanalytik (Übersichtsbericht). Fresenius Z. Anal. Chem. 1985;320:423-428.
32. Weiss J. Handbook of Ion Chromatography. Wiley VCH- Verlag, Germany; 2016.
33. Forti JC, Rocha RS, Lanza MRV, Bertazzoli R. Electrochemical synthesis of hydrogen peroxide on oxygen-fed graphite/PTFE electrodes modified by 2-ethylanthraquinone. Journal of Electroanalytical Chemistry. 2007;601:63–67.
34. Ribeiro MCE, Couto AB, Ferreira NG, Baldan MR. Nitrate Removal by Electrolysis Using Cu/BDD Electrode Cathode. ECS Transactions. 2014;58:21-26.
35. Hasnat MA, Agui R, Hinokuma S, Yamaguchi T, Machida M. Different reaction routes in electrocatalytic nitrate/nitrite reduction using an H+-conducting solid polymer electrolyte. Catalysis Communications. 2009;10:1132-1135.
36. Hasnat MA, Amirul Islam M, Borhanuddin SM, Ullah Chowdhury MR, Machida M. Influence of Rh on electrocatalytic reduction of NO3- and NO2- over Pt and Pd films. Journal of Molecular Catalysis A: Chemical. 2010;317:61-67.

37. Szpyrkowicz L, Daniele S, Radaelli M, Specchia S. Removal of NO3- from water by electrochemical reduction in different reactor configurations. Environmental. 2006;66:40-50.

38. Katsounaros I, Dortsiou M, Kyriacou G. Electrochemical reduction of nitrate and nitrite in simulated liquid nuclear wastes. Journal of Hazardous Materials. 2009; 171:323-327.



*Peer-review history:*
*The peer review history for this paper can be accessed here:*
*http://www.sciencedomain.org/review-history/26746*